Lawrence Berkeley National Laboratory
LBL Publications

Title

Control of Interfaces for TEM Analysis

Permalink

https://escholarship.org/uc/item/7rv3k5s8

Authors

Dahmen, U
Westmacott, K H

Publication Date

1989-06-01

eScholarship.org Powered by the California Digital Library
University of California

LBL-27259
Preprint

Lawrence Berkeley Laboratory
UNIVERSITY OF CALIFORNIA

Materials & Chemical Sciences Division

National Center for Electron Microscopy

Submitted to Journal of Electron Microscopy Technique

Control of Interfaces for TEM Analysis

U. Dahmen and K.H. Westmacott

June 1989

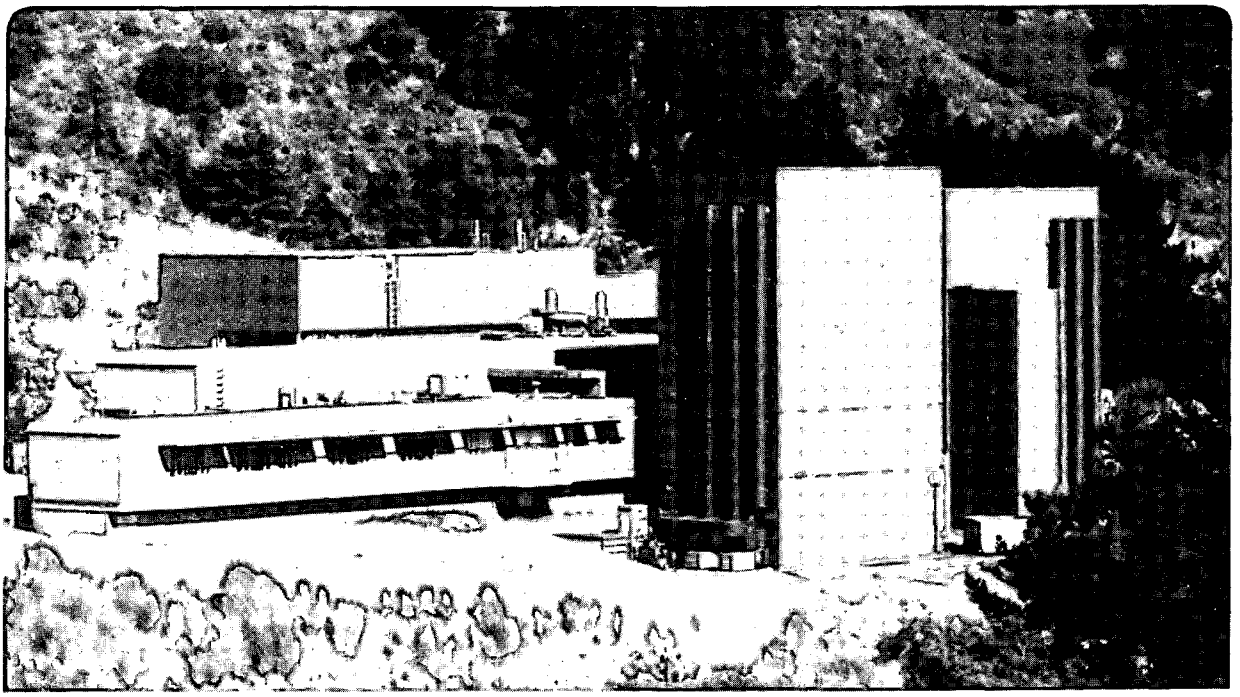

Prepared for the U.S. Department of Energy under Contract Number DE-AC03-76SF00098.

| LOAN COPY |
|Circulates |
|for 2 weeks|
Bldg. 50 Library.
Copy 2
LBL-27259

DISCLAIMER

This document was prepared as an account of work sponsored by the United States Government. While this document is believed to contain correct information, neither the United States Government nor any agency thereof, nor the Regents of the University of California, nor any of their employees, makes any warranty, express or implied, or assumes any legal responsibility for the accuracy, completeness, or usefulness of any information, apparatus, product, or process disclosed, or represents that its use would not infringe privately owned rights. Reference herein to any specific commercial product, process, or service by its trade name, trademark, manufacturer, or otherwise, does not necessarily constitute or imply its endorsement, recommendation, or favoring by the United States Government or any agency thereof, or the Regents of the University of California. The views and opinions of authors expressed herein do not necessarily state or reflect those of the United States Government or any agency thereof or the Regents of the University of California.

CONTROL OF INTERFACES FOR TEM ANALYSIS

U. Dahmen and K. H. Westmacott
National Center for Electron Microscopy, Lawrence Berkeley Laboratory,
University of California, Berkeley, CA 94720.

ABSTRACT

A full understanding of the nature and properties of interfaces through comprehensive transmission electron microscopy analysis is an important goal in many materials science problems. In the present paper methods for manipulating microstructures and techniques for optimizing imaging conditions are described for several model systems.

INTRODUCTION

Techniques for interface characterization by TEM are well developed. It is now possible to determine the local structure of grain boundaries and heterophase boundaries in great detail. However, due to variations in interface orientation and structure it is often impossible to perform complete and concise analyses of interfaces that are typical for a given alloy or crystallography. Moreover, due to the difficulty and tediousness of completing a comprehensive TEM analysis it is impractical to examine a statistically significant sample of interfaces necessary to characterize the typical structure. It is therefore important to use all means available to produce microstructures with a minimum of variation in interface structure to ensure that only typical interfaces are analyzed.

In the present contribution several examples are outlined in which interface analyses have been simplified by taking advantage of symmetry properties inherent in solid state reactions, and by using special heat treatments, and thin film deposition techniques to produce optimum samples.

FCC-BCC INTERFACES IN Cu-Cr

The structure of the interface between fcc and bcc materials has been a subject of intense interest in the past 15 years, e.g.[1-8]. Dilute Cu-Cr alloys have been studied in detail since it is a model system for fcc/bcc transformation crystallography with almost no volume change. One of the difficulties that plagued these investigations

was the fact that the morphologies of the overaged Cr precipitates were extremely variable [9-11]. Interfaces were often curved rather than planar, and as a result the interface structure varied continuously.

It was subsequently found that a much more consistent morphology of needle or lath shaped precipitates could be obtained in the same alloy by a quench/age rather than a direct quench treatment [12,13]. Fig. 1 shows a distribution of precipitates typical for this heat treatment. The direction of the laths was determined by stereographic trace analysis and confirmed by symmetry-assisted analysis to be near <761> of the Cu matrix [14]. The orientation relationship was very close to the Kurdjumov-Sachs relationship with close-packed planes and directions almost parallel.

Further overaging led to larger precipitates with the same basic morphology. It is likely that these laths are closer to their equilibrium morphology, and because of their higher consistency their characterization is greatly facilitated.

Fig. 2 shows a conventional contrast analysis of one such lath. When the lath is seen nearly edge-on the planar facets on the broad interface are clearly apparent (fig. 2a). When inclined to the beam these facets show an interfacial structure that is dominated by a single set of parallel striations along the long axis of the lath (fig. 2b). The spacing of these striations depends on the plane of the facet and position in the interface, and their variation is most clearly visible at the curved ends of the particle. In agreement with the hypothesis that needles and laths lie along invariant line directions [14], these striations are analyzed as the slip traces, or dislocation lines of the lattice-invariant shear that accommodates the structural change. In the curved interface at an angle to the habit plane of the laths, the dislocation spacing is very small, and due to the absence of a long range strain field their contrast is extremely weak. It is thus necessary to use high resolution techniques to analyze these interfaces in more detail.

Fig. 3 is a high resolution micrograph showing a section of such an interface viewed along the $<110>_{Cu}/<111>_{Cr}$ common close-packed direction. The <761> axis of the lath lies at 7.5° from this direction and thus only the $\{\bar{1}11\}$ sections of the interface would be precisely on-edge in the <110> orientation. In contrast, the section shown in Fig. 3 is rotated about 8° from $\{\bar{1}11\}$ and is thus inclined ~1° with respect to the <110> beam direction. The horizontal rows of bright dots (marked by arrows) on the common close packed planes are the same features as the <761> striations in Fig. 2. Their projected length is ~2nm, corresponding to a foil thickness of ~15nm. To see

these features end-on it is necessary to tilt the crystal away from the low-index zone axis condition.

Fig 4 illustrates the problem more clearly: a Cr needle is seen nearly end-on along the common close-packed direction. The projected width of the interface in this phase contrast image shows that the particle is slightly inclined to the beam. Only a limited part of the curved interface (see arrow) is on edge, but in any case this is usually not the interface facet of interest. The interface shown in Fig. 3 is of a similar section, and its structure is therefore only of secondary importance to the main goal of understanding the structure of the planar sections of the interface.

Due to the limited specimen area visible in a high resolution micrograph it is desirable to examine particles that are small enough to be entirely visible in one micrograph. It is then possible to examine the whole interface instead of only selected sections. Thus to produce smaller particles the alloys were overaged at a lower temperature. After this heat treatment (see Fig 4), the particles were about 60nm in cross section and clearly faceted. An analysis of such small faceted particles can provide valuable information on the correlation between the interface structure of different facets and their connection with the orientation relationship and morphology of a single particle.

To reiterate, the best orientation for the study of a needle- or lath interface is one where the beam is exactly parallel to the lath axis. At this orientation the entire interface is seen on edge. However, in order to see structure images on both sides of the boundary it is necessary to go to the nearest zone axis orientation where generally the interface will no longer be on edge[15]. The structure of the interface will then have to be synthesized from the combined information of several high resolution and conventional contrast experiments. It is clear that in order to perform such an experiment it is first necessary to produce a microstructure whose scale and degree of consistency facilitates the experimental analysis and allows its comparison with calculated interface structures.

Al-Ge ALLOYS

Al-Ge is an alloy system that fulfills the necessary crystallographic conditions for direct analysis, i.e. that the interface be on edge and both crystals be simultaneously in zone axis orientations[16]. Needle- or lath-shaped precipitates form along <100> and <110> directions of the Al matrix in a characteristic microstructure such as that shown in fig. 5. Examination of these laths in cross-section reveals an interesting internal defect structure of multiple twins[17,18]

whose disposition is reflected in the external shape of the particle[19]. An example of such a lath is shown in fig. 6. Because in this image the interface, as well as the two low index zone axes, are accurately parallel to the beam it is possible to see the orientation relationship, interface structure and internal defect structure within a single micrograph. Note that this special orientation relationship is inherent to the alloy system used and cannot be influenced by heat treatment. However, the heat treatment conditions do allow control over the size of the particles, and it is possible to grow precipitates to a size that allows examination of a closed interface rather than a single planar interface such as is commonly seen in cross-section samples of thin films on a substrate.

Close examination of such interfaces, shown enlarged in Fig. 7, reveals that only very limited atomic relaxation has occurred. Fig. 7a shows a section of the commonly found $\{111\}_{Ge}$ facet which lies almost, but not quite, parallel to $\{310\}_{Al}$. Even though for this commonly observed orientation relationship the vertical $\{111\}_{Ge}$ and $\{100\}_{Al}$ planes are parallel, there is no evidence of elastic accommodation of the differential in spacing of these parallel planes and the structures of both the Al matrix and the Ge precipitate remain basically undisturbed up to one atomic layer of the boundary. No long-range distortions, dislocations or structural relaxation units can be made out, a characteristic typical of an incoherent interface. This is even more apparent in the interface section shown in Fig. 7b. The Ge crystal is twin-related to that shown in Fig. 7a and thus its orientation relationship with the Al matrix is one in which, apart from the common zone axis, no low-index directions are aligned. Although these interfaces show no signs of atomic relaxations it is likely that some structural rearrangement does take place in the atomic layers immediately adjacent to the boundary, and the possibility of interface reconstruction is presently under study.

Twinned Ge precipitates with more complex substructure are found frequently. A typical example is given in Fig. 8. These pentagonally-twinned particles are believed to develop by vacancy-assisted nucleation in segment 3 followed by a growth sequence during which the precipitate undergoes repeated twinning[20]. The final cross-sectional shape of the needle will depend on the sequence in which the twinning occurs and the segments in which the coherency strains are accommodated by either elastic or plastic deformation. These strains arise because the five twins sharing the common <110> zone axis are coherently compatible only if they are strained to fill up the residual 7.5° gap that arises when five twin segments of 70.5° angle are joined at a common apex. The measurable

relative misorientation of the vertical {111} planes betweeen segments 1 and 1a shows that some of the necessary accommodation has taken place by repeated twinning between these two segments.

Precipitation reactions with special crystallography such as that found in Al-Ge alloys are presently being used by a number of groups to study metal-ceramic interfaces in model alloy systems by high resolution microscopy[21-23],.

Al-Cu ALLOYS

Al-Cu alloys are known to form precipitate structures of (bct) θ' plates on {100} planes of the (fcc) matrix. The structure of the broad interface is relatively simple and well-understood[24,25]. Because of the good atomic fit across this interface it is usually found to be atomically flat, and thickening of the plates must proceed by a ledge mechanism. For this reason the structure of the edges of the precipitates and of growth ledges on the broad interfaces is of primary interest. It has been shown that during thickening, plates tend to take on discrete thicknesses[26]. This was related to the matching in the {100} plane spacing between matrix and precipitate normal to the plate. However, this model could not explain the observation that no plates under a thickness of two unit cells were found. Subsequently it was suggested that growth units occurred in pairs to accommodate shear transformation strains[27]. This led to the prediction that a single unit cell thick plate could be created by glide or climb of a 1/2<100> partial dislocation on an {001} plane. In order to test this hypothesis, heterogeneous nucleation of θ' on dislocations was examined. A direct-quench heat treatment is known to lead to the formation of concentric series of vacancy dislocation loops by the operation of Bardeen-Herring climb sources[28-30]. As these loops expand on {110} planes they trigger the heterogeneous nucleation of two of the three variants of θ' precipitates. Six such colonies can form on the six crystallographically equivalent {110} planes and the interaction of different sets lead to intriguing intergrowths such as the one shown in fig. 9.

By close examination of the mechanism of nucleation it was found that the existing 1/2<110> edge dislocation kinks onto a {100} plane and then dissociates into a 1/2<100> leading partial and a 1/2 <010> trailing partial[31]. This dissociation is readily apparent in a weak beam analysis of a segment of one of the dislocation loops, shown in fig. 10. The kinking of the climb loop from its {110} plane onto {100} and {010} planes can be seen where the precipitates are attached to the dislocation line. Notice a change in thickness of the precipitate marked by an arrow, visible as a change in the weak displacement fringe contrast. Several precipitates have already

pinched off the dislocation and at these positions the loop has unkinked and returned to its original {110} plane. The shape of these precipitates is that of a small circular plate. These are ill-suited for edge-on examination by high resolution microscopy since the edges of the particle will be curved along the beam direction, leading to a confused image.

The study of the edges of θ' particles by atomic resolution imaging requires that these edge be straight and lie along <100> directions. Instead of examining many different particles in order to find one that has by chance the correct interface segment, it is possible to modify the heat treatment so as to promote faceting. Fig. 11 shows a dark field image of a θ' particle formed by long term aging at low temperature. When such plates are examined at high resolution (see fig. 12) the structure at their edge is clearly visible without artifacts from partial overlapping of matrix and precipitate. A dislocation seen as an extra half plane is visible at the position of the arrow at the very edge of the particle. The long range elastic distortion of the Al lattice around the edge of the particle as well as the localized elastic distortion field within a few atomic spacings immediately adjacent to the edge are readily apparent.

Thus, in this alloy system also, the precipitate structures can be tailored by an appropriate choice of heat treatment to match the requirements of an optimized TEM analysis.

GRAIN BOUNDARIES IN Al THIN FILMS

The characterization of grain boundary structure in close-packed metals at a level of resolution that allows comparison with theoretical predictions remains one of the greater challenges to the experimentalist. One approach has been to examine boundaries and their dislocation substructures in polycrystals by diffraction contrast techniques. However, because of their random nature the information obtained on a particular boundary is usually of limited value. A more common approach is based on the careful control of both the bicrystal orientation and boundary plane, but the task of producing a suitable specimen is difficult and tedious. Boundaries produced in this manner have been the most useful in providing experimental data to compare with theory[32]. However, as each sample contains only one boundary the statistical sampling has been limited to special boundaries of low Σ values.

An alternative technique for the controlled formation of grain boundaries with fixed misorientation based on the heteroepitaxial growth of thin films has

recently been pointed out. It was shown that when Al deposits in two crystallographically equivalent orientations on a {100} Si surface it forms a continuous bicrystal structure with the two crystals separated by 90° <110> tilt boundaries[33,34]. Furthermore, an intermediate temperature anneal of this film leads to the preferential reorientation of the boundary planes (at fixed misorientation of ~ 90°) into low-energy facets. This is illustrated in Fig. 13 with a pair of bright field micrographs taken under mirror-related two-beam conditions. The planar facets in the Al preferentially adopt the symmetrical $\{557\}_1/\{55\bar{7}\}_2$ and the asymmetrical $\{100\}_1/\{011\}_2$ boundary orientation, which they inherit from the mirror planes of the Si substrate crystal. An example of a high resolution image showing an asymmetrical $\{100\}_1/\{011\}_2$ boundary is seen in Fig 14. This interface is bounded by low-index planes on both sides, and the 90° misorientation between the two adjacent grains is immediately apparent. Local atomic relaxations are visible in some areas (see arrows), but due to the fact that the repeat periods of the lattices parallel to the boundary are in the ratio of $1/\sqrt{2}$, the lattices are incommensurate and this boundary cannot be periodic[35]. Complete characterization of other such boundaries and comparison with atomistic calculations is currently underway. However, it is already apparent that the unique configuration of the continuous bicrystal structure will allow accurate measurements of grain boundary structure and behavior to be made by both high resolution and in-situ electron microscopy[36].

SUMMARY AND CONCLUSIONS

In the characterization of interfaces by TEM it is essential to exploit any means of controlling the interface geometry to facilitate the analysis and make possible the direct comparison between theoretical models and experimental data. Several examples illustrated how manipulation of both homophase and heterophase interfaces have led to successful analyses. The common goal has been to provide a clean, well-equilibrated planar boundary with well-defined, reproducible crystallography, on a scale that allows meaningful characterization by TEM. In the case of Cu-Cr alloys this was achieved by quench-aging, in Al-Cu alloys by direct-quenching or by long-term aging at low temperature, in Al-Ge through natural topotaxial relationships and in Al bicrystals through heteroepitaxial thin film growth and subsequent annealing treatments.

While randomly produced microstructures continue to be in great need of experimental characterization, the most rapid advancement in the scientific

understanding of interfaces is likely to come about by directly comparing experimental and theoretical special boundaries that can be engineered by use of techniques such as the ones outlined above.

ACKNOWLEDGMENT

This work is supported by the Director, Office of Energy Research, Office of Basic Energy Sciences, Materials Sciences Division of the U.S. Department of Energy under contract No. DE-AC03-76SF00098.

FIGURE CAPTIONS

Fig.1 HVEM micrograph showing even distribution of <761> Cr laths in a quench-aged Cu-Cr alloy. Random appearance of lath axes is due to the multiplicity of 24 equivalent <761> directions.

Fig. 2 Dark field contrast analysis of overaged Cr lath; (a) habit plane edge-on and common close-packed planes in diffraction condition and (b) inclined interface with matrix only in diffraction condition, showing finely spaced striations along lath axis.

Fig. 3 High resolution micrograph of special section of interface between overaged Cr lath (bottom) and Cu matrix (top) viewed along $<110>_{Cu}/<111>_{Cr}$ common close-packed direction, 7.5° from <761> lath axis. $\{111\}_{Cu}/\{110\}_{Cr}$ common close-packed planes are horizontal; arrows point to interface dislocations along <761> axis spaced about 2nm apart.

Fig. 4 Phase contrast image of faceted Cr lath or needle seen along common close-packed direction, showing small cross section, inclined interface, periodic dislocation structure and planar facets.

Fig. 5 HVEM micrograph illustrating characteristic distribution of <100> laths of Ge in Al matrix. Moiré fringes due to alignment of $<110>_{Ge}$ and $<100>_{Al}$ along lath axis. Zone axis <001>.

Fig. 6 High resolution micrograph of typical Ge needle seen along its axis illustrating orientation relationship, multiple twinning, cross section shape and interface structure of the precipitate.

Fig. 7 Atomic resolution images of interface sections of particle shown in fig. 6. Absence of long range elastic distortions in precipitate or matrix is apparent for both the typical faceted interface across which low-index $\{200\}_{Al}/\{111\}_{Ge}$ planes are parallel (a) and the more random, curved interface with no alignment of low-index planes (b).

Fig. 8 Pentagonally-twinned Ge needle in Al matrix viewed end-on, with five twin segments labeled. Parallel twin bands in segments 1 and 5 serve to accommodate internal misfit strain as seen from misalignment between vertical {111} planes in segments 1a and 1. (micrograph by J. Douin).

Fig. 9 Bird-shaped intergrown colonies of θ' precipitates heterogeneously nucleated on climbing dislocation loops in direct-quenched Al-Cu alloy.

Fig. 10 Contrast analysis of heterogeneous nucleation of θ' plates on segment of {110} dislocation loop. Edge-on view of {110} loop plane in (c) shows dislocation kinking onto specific {100} plane where attached to a precipitate.

Fig. 11 Dark field image of θ' plate showing faceting after long-term low-temperature aging. Note also antiphase boundaries.

Fig. 12 High resolution micrograph of faceted θ' precipitate plate in Al-Cu alloy seen edge-on.Extra half plane terminating at top left corner of the plate marked by arrow, (courtesy MRS).

Fig. 13 Continuous bicrystal structure of Al thin film deposited on {100} Si with 90° misorientation between the two intertwining grains. Complementary images in (a) and (b) recorded in bright field under mirror-related two-beam conditions.

Fig. 14 High resolution micrograph of asymmetrical 90° <110> tilt boundary in continuous bicrystal Al film produced by ionized cluster beam deposition. Arrows show localized atomic relaxation, (courtesy MRS, micrograph by C.J.D. Hetherington).

REFERENCES

1. G. Bäro and H. Gleiter, Acta Met. 21, 1405, (1973)
2. G. Bäro and H. Gleiter, Acta Met. 22, 141, (1974)
3. K.C. Russell, M.G. Hall, K.R. Kinsman and H.I. Aaronson, Met. Trans. 5, 1503 (1974)
4. W. Bollmann, phys. stat. sol. (a) 21, 543 (1974)
5. J.M. Rigsbee and H.I. Aaronson, Acta Met. 27, 351 (1979)
6. R.C. Ecob and B.Ralph, Acta Met. 29, 1037 (1981)
7. C.P. Luo and G.C. Weatherly, Acta Met. 35, 1963 (1987)
8. C.P. Luo and G.C. Weatherly, Phil. Mag. 58, 445(1988)
9. M.G. Hall, H.I. Aaronson and K.R. Kinsman, Surface Sci. 31, 257 (1972)
10. M.G. Hall and H.I. Aaronson, Acta Met. 34, 1409 (1986)
11. M.G. Hall, J.M. Rigsbee and H.I. Aaronson, Acta Met. 34, 1419 (1986)
12. G.C. Weatherly, P. Humble and D. Borland, Acta Met. 27, 1815 (1979)
13. U. Dahmen, M.J. Witcomb and K.H. Westmacott, Scr. Met. 22, 1867 (1988)

14. U. Dahmen, P. Ferguson and K.H. Westmacott, Acta Met. 32, 803 (1984)
15. U. Dahmen, J. Douin, C.J. Hetherington and K.H. Westmacott, MRS Symp. Proc. on High Resolution Microscopy of Materials, Boston (1988)
16. K.H. Westmacott and U. Dahmen, Proc. Int. Conference on *Phase Transformations '87*, in press
17. U. Köster, Mat. Sci. Eng. 5, 174 (1969)
18. G.N. Gouthama, Subbana and Kishore, Mat. Sci. Forum 3, 261 (1985)
19. U. Dahmen and K.H. Westmacott, Science 233, 875 (1986),
20. J. Douin, U. Dahmen and K.H. Westmacott, submitted to Phil. Mag.
21. W. Mader, Z. Metallk. submitted
22. W. Mader, MRS Proc. 82, 403 (1987)
23. P. Pirouz and F. Ernst, Acta/Scr. Met Conf. on Metal/Ceramic Interfaces, in press
24. C. Laird and H.I. Aaronson, Trans. Met. Soc. AIME, 242, 1393 (1968)
25. R. Sankaran and C. Laird, Phil Mag. 29, 179 (1974)
26. W.M. Stobbs and G.R. Purdy, Acta Met. 26, 1069 (1978)
27. U. Dahmen and K.H. Westmacott, phys. stat. sol. (a) 80, 249 (1983)
28. P. Guyot and M. Wintenberger, J. Mat. Sci. 9, 614 (1974)
29. T.J. Headley and J.J. Hren, Phil. Mag. 34, 101 (1976)
30. T.J. Headley and J.J. Hren, J. Mat. Sci. 11, 1867 (1976)
31. U. Dahmen and K.H. Westmacott, Scr. Met. 17, 1241 (1983)
32. R.W. Balluffi, M. Rühle and A.P. Sutton, Mat. Sci. and Eng. 89, 1 (1987)
33. U. Dahmen and K.H. Westmacott, Scr. Met. 22,1673 (1988)
34 C.B. Carter, Acta Met. 36, 2753 (1988)
35 A.P. Sutton, Acta Met. 36, 1291 (1988)
36. K.H. Westmacott and U. Dahmen, Proc. ISIAT Conference, Tokyo, (1989), in press

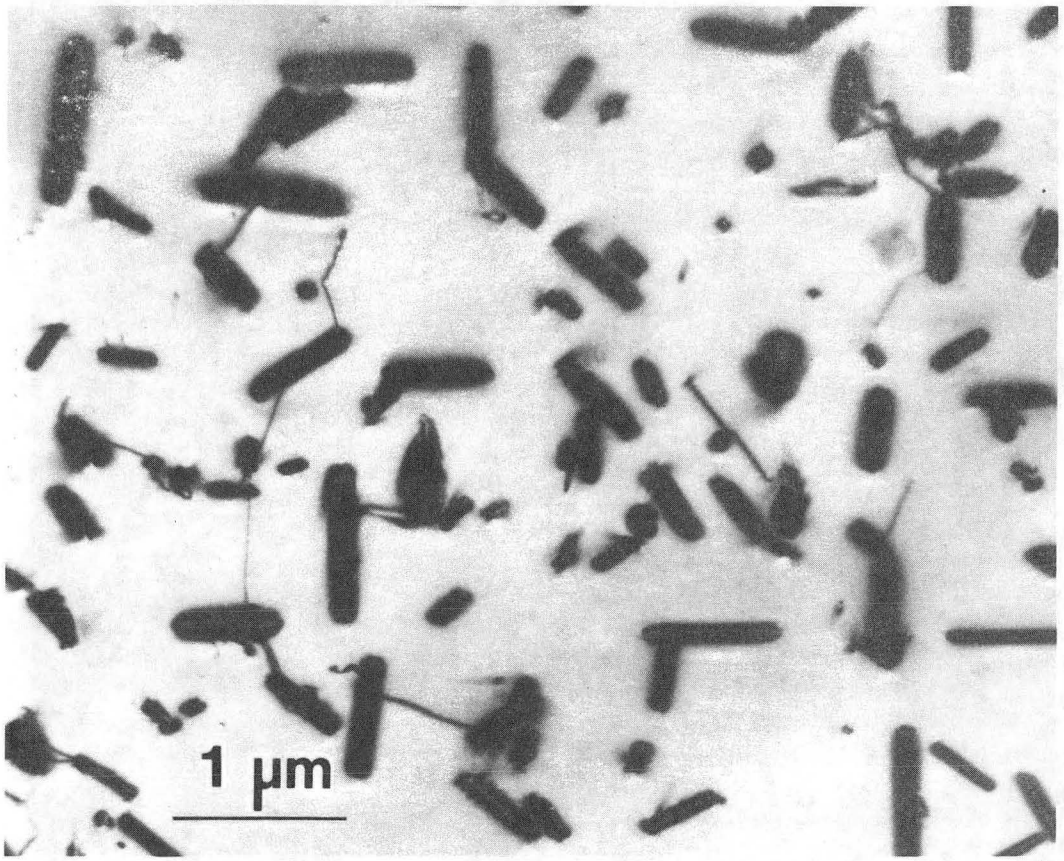

XBB 865-3759

FIGURE 1

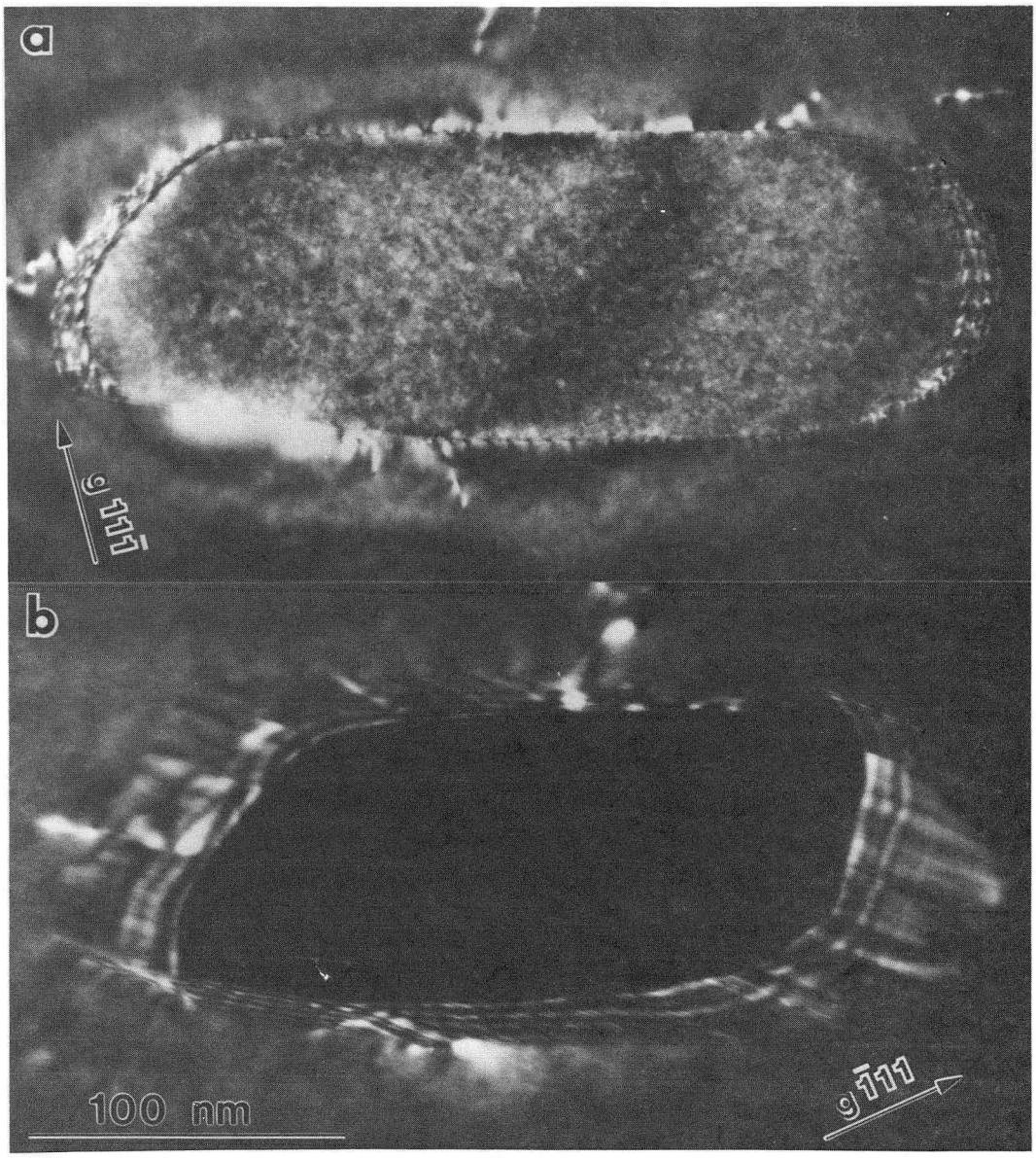

XBB 894-3385

FIGURE 2

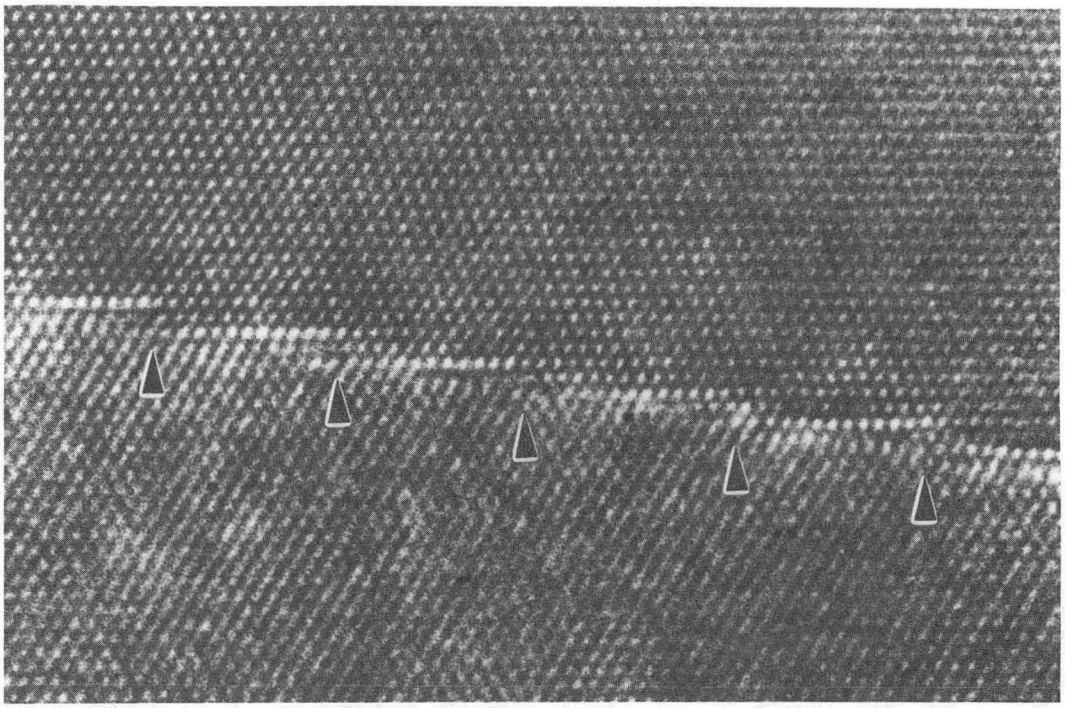

XBB 894-3384

FIGURE 3

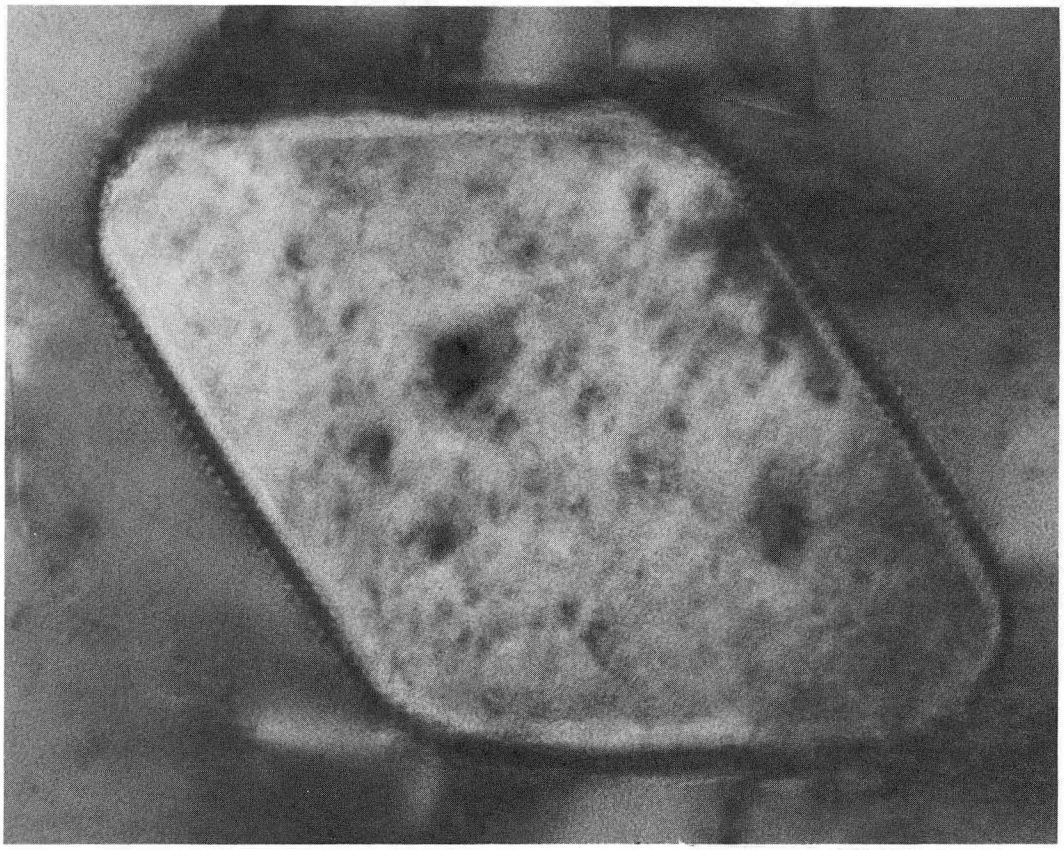

XBB 889-8855

FIGURE 4

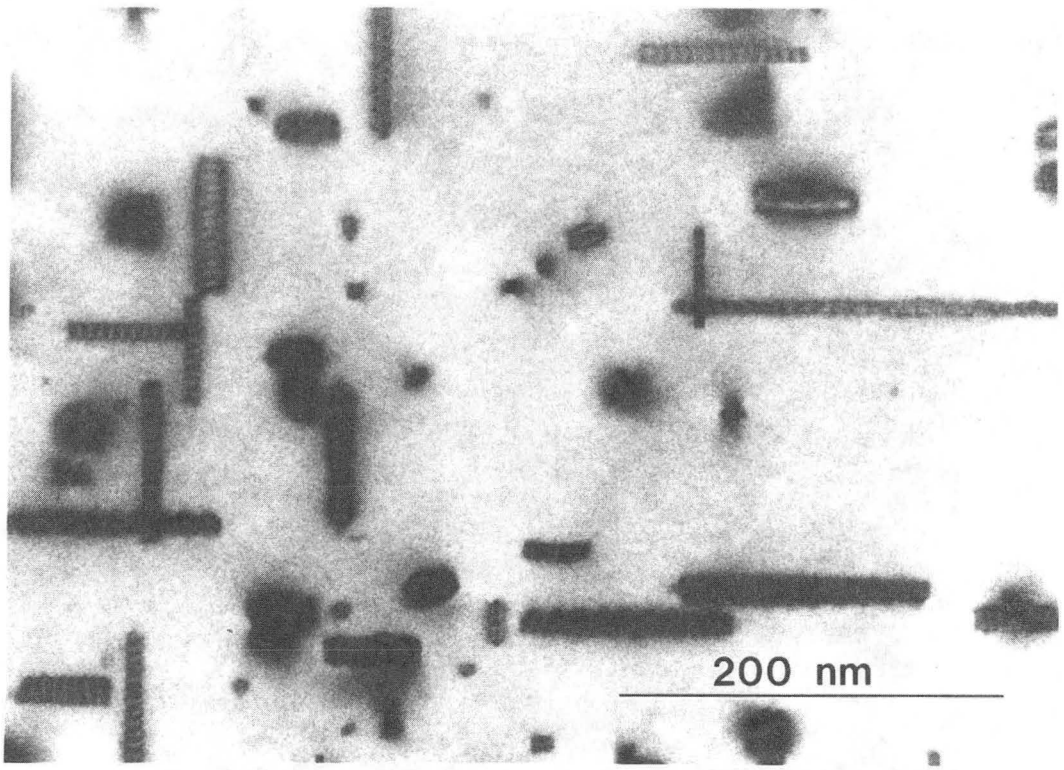

XBB 894-3381

FIGURE 5

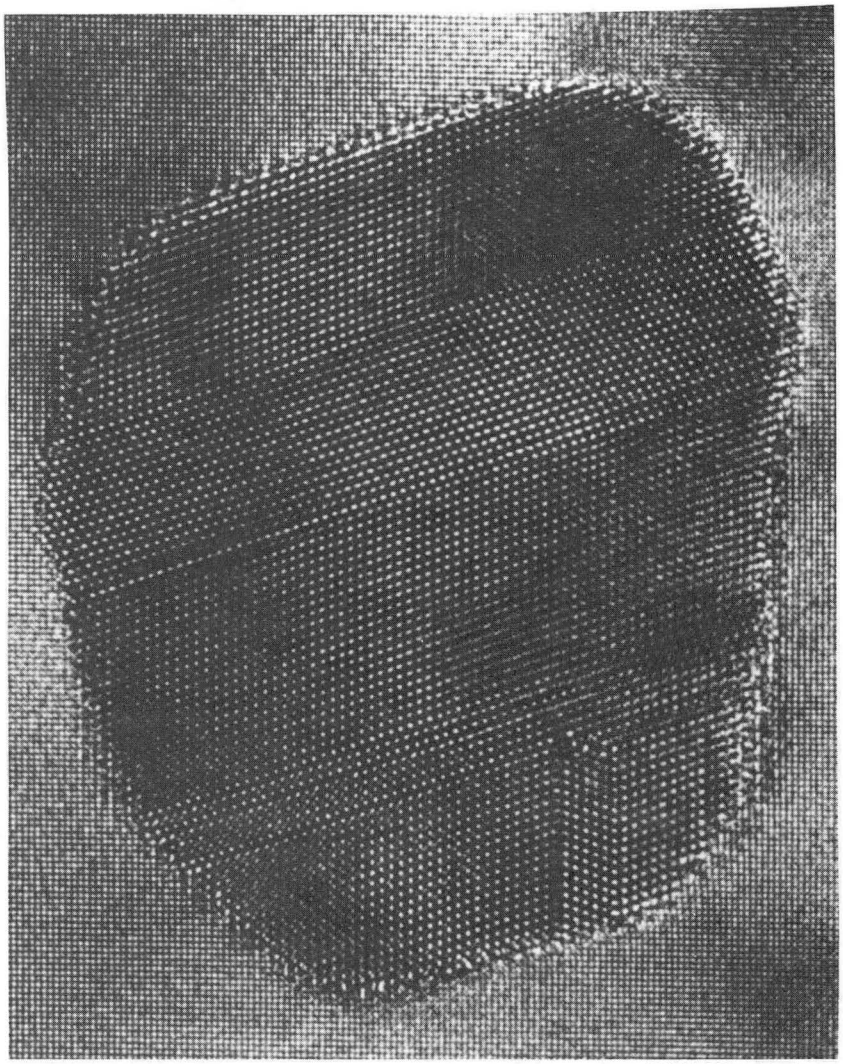

XBB 895-4158

FIGURE 6

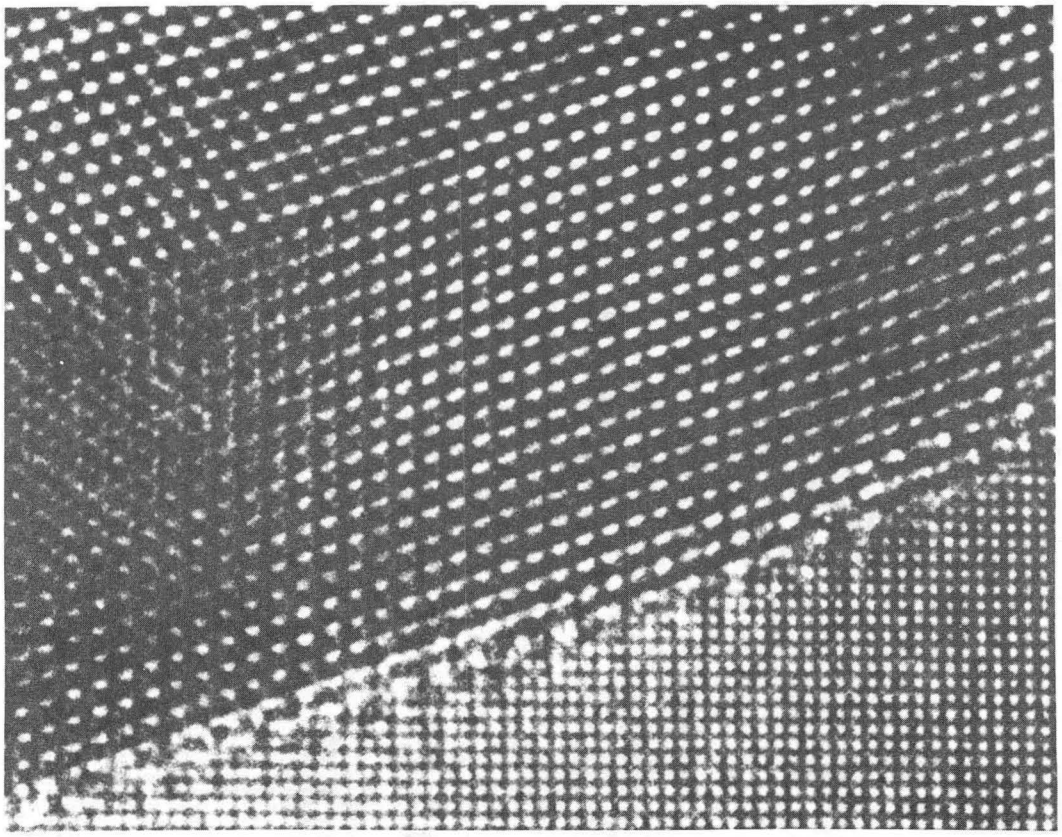

XBB 895-4157

FIGURE 7a

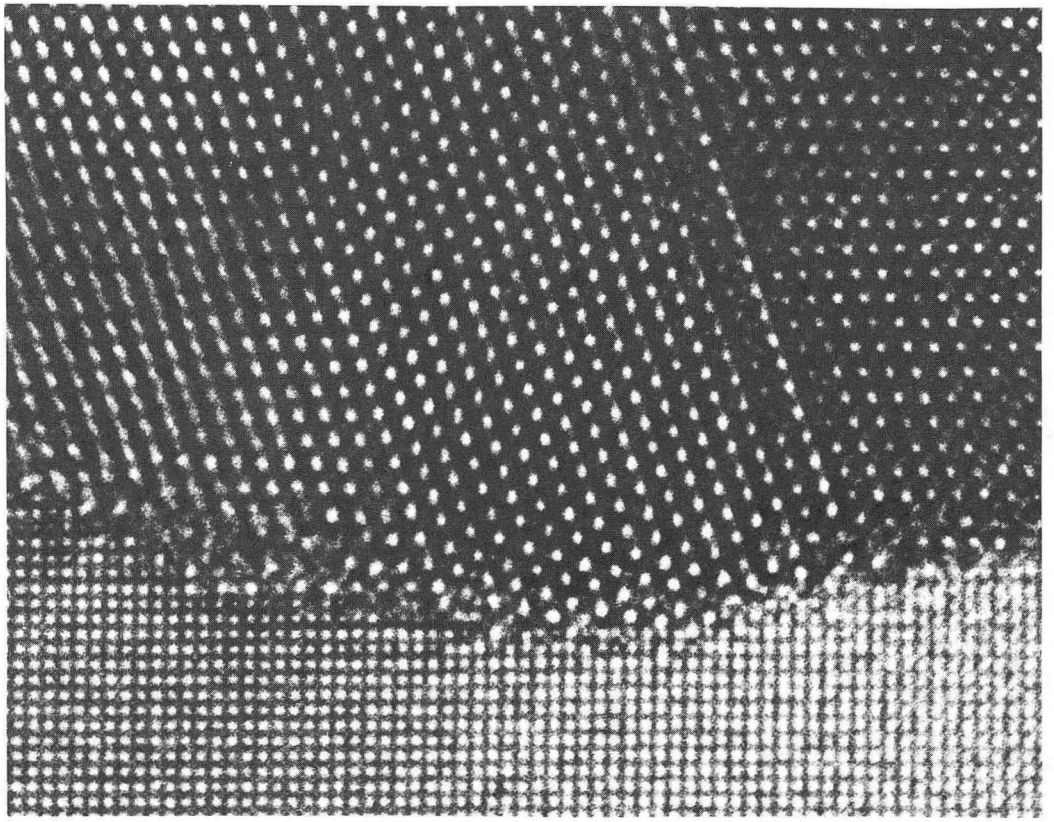

XBB-895-4156

FIGURE 7b

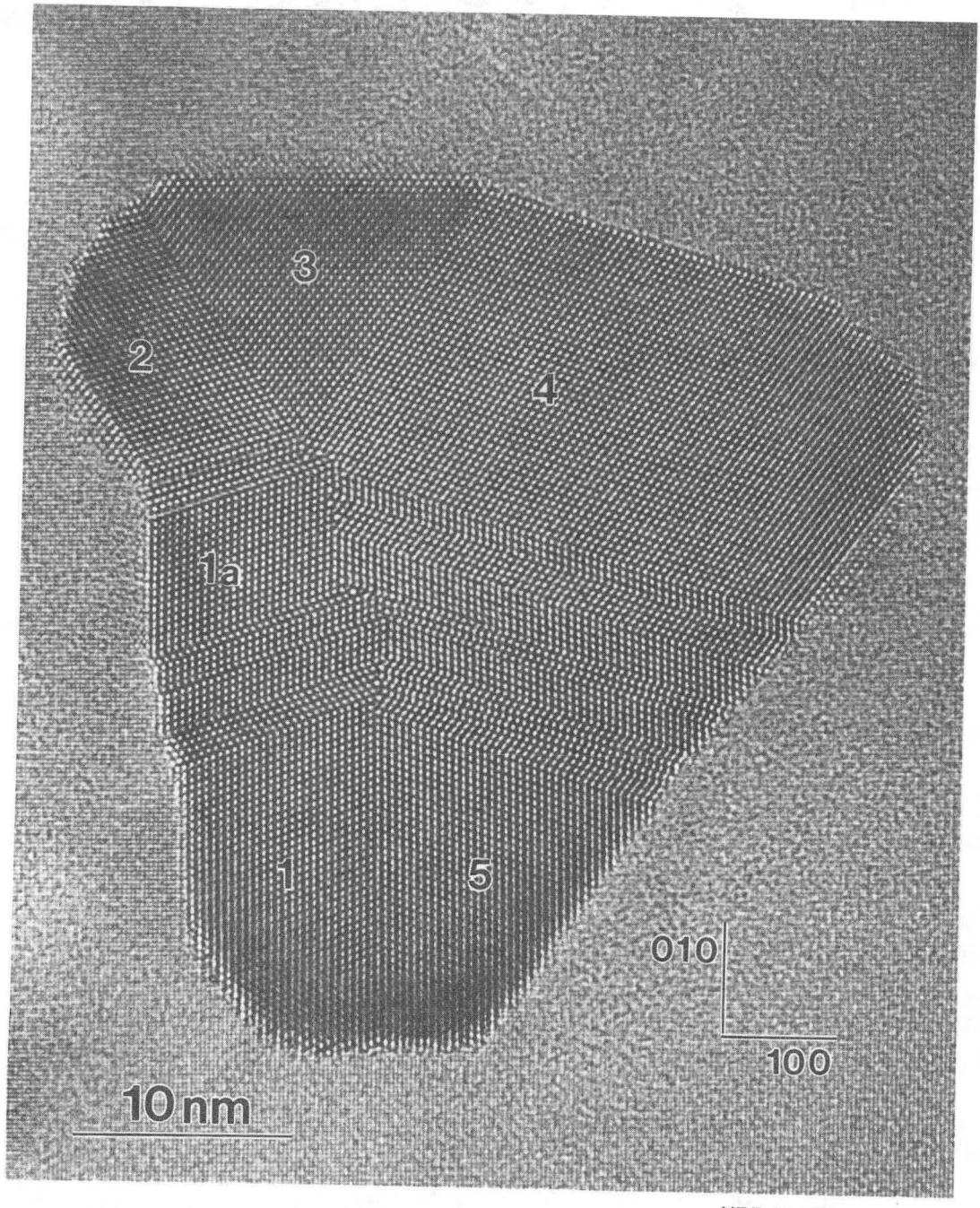

XBB 894-3383

FIGURE 8

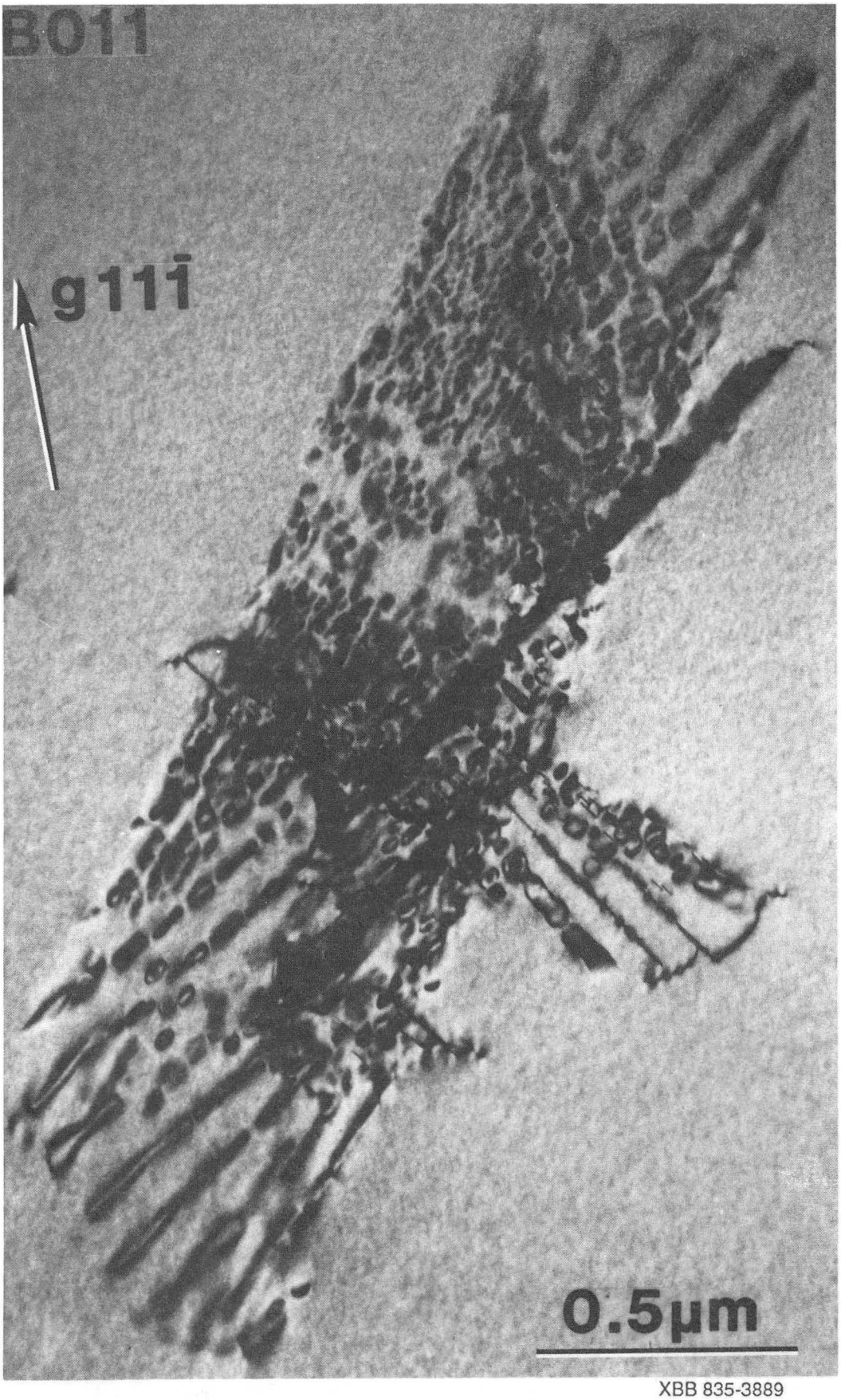

XBB 835-3889

FIGURE 9

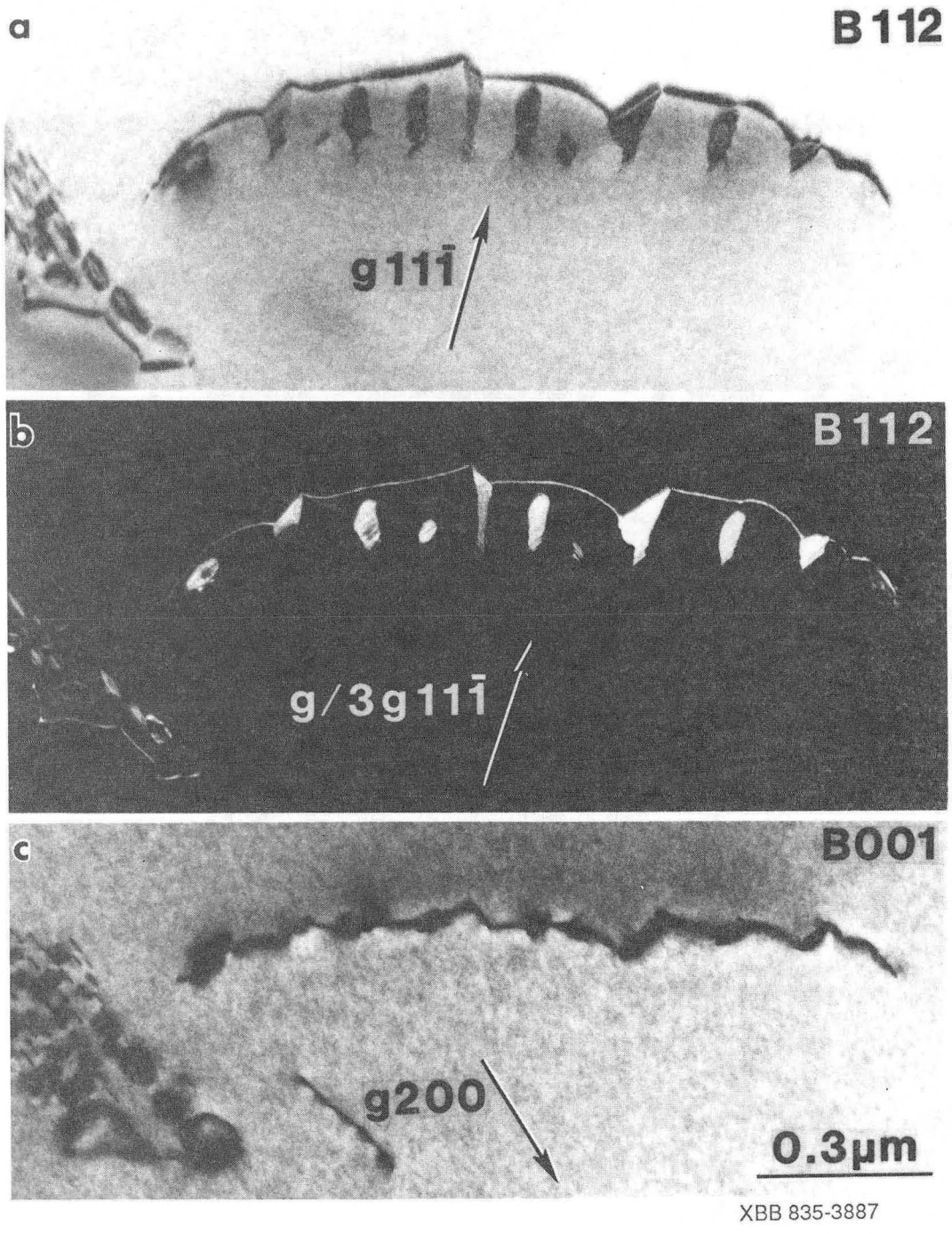

XBB 835-3887

FIGURE 10

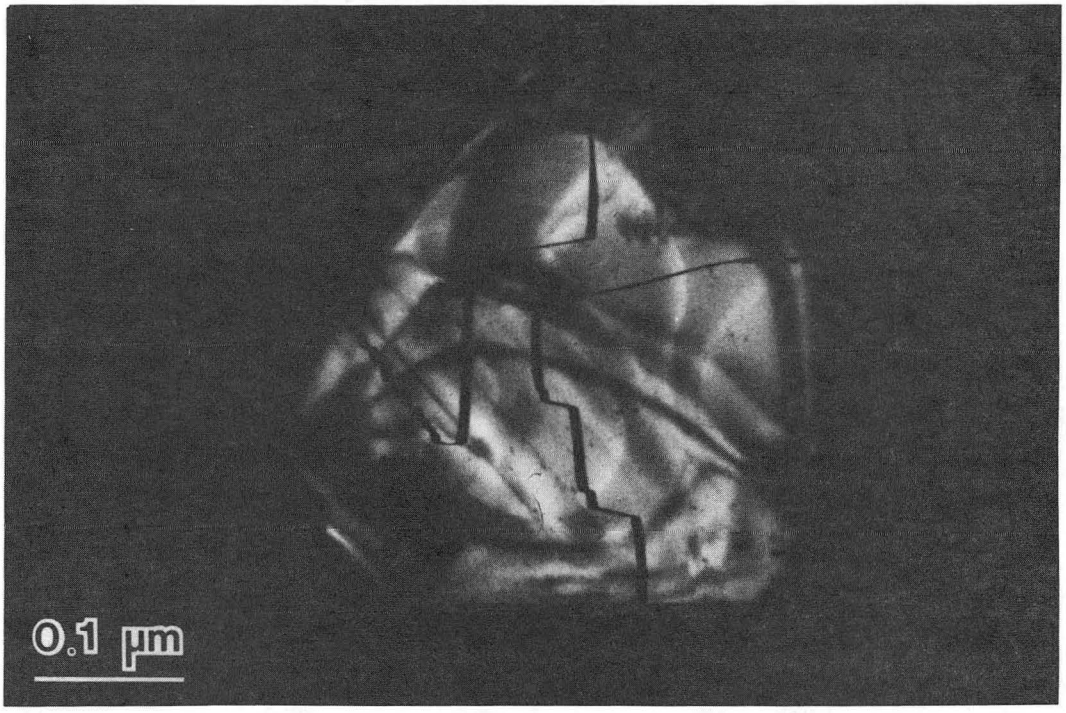

FIGURE 11

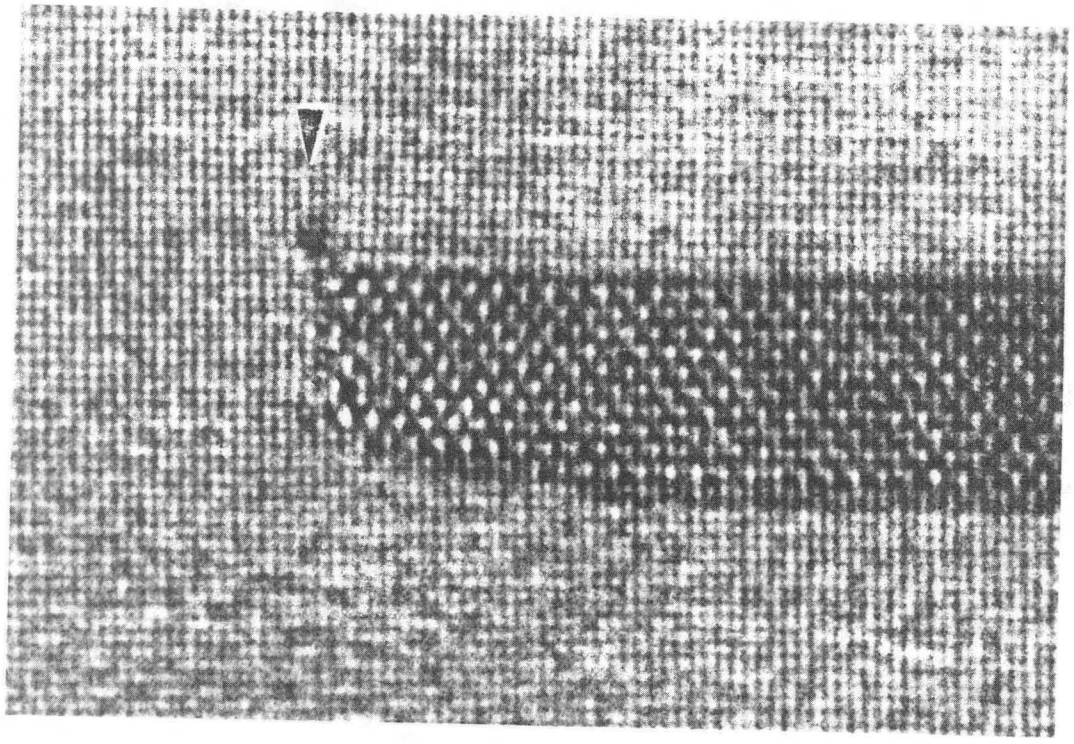

XBB 894-3380

FIGURE 12

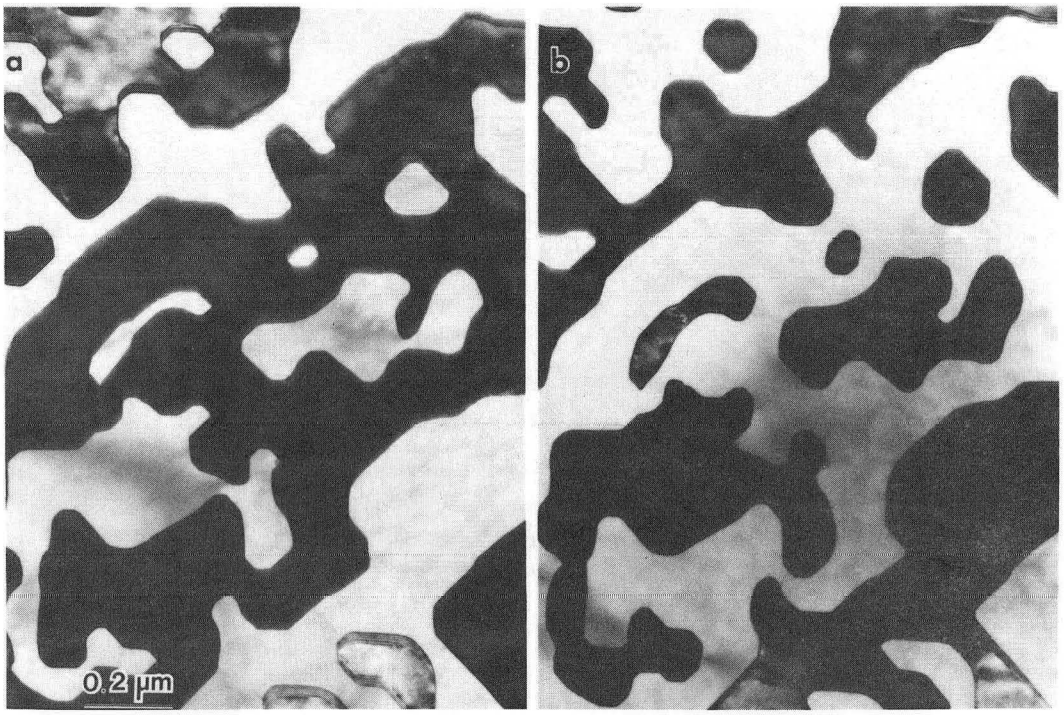

XBB 880-10325

FIGURE 13

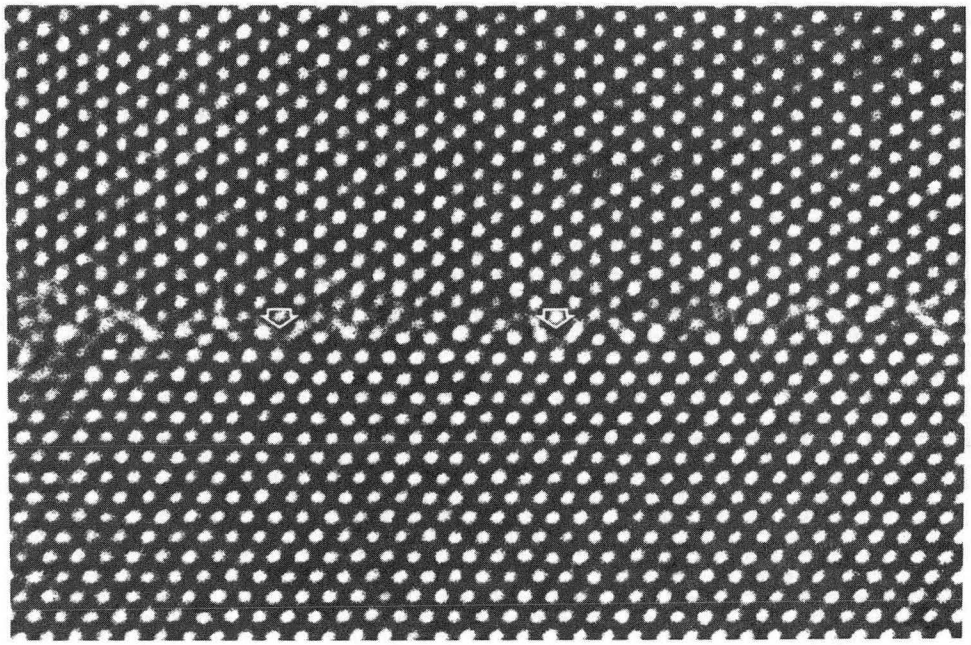

XBB-880-10319

FIGURE 14

LAWRENCE BERKELEY LABORATORY
TECHNICAL INFORMATION DEPARTMENT
1 CYCLOTRON ROAD
BERKELEY, CALIFORNIA 94720